Rare Met. (2018) 37(2):118–122
https://doi.org/10.1007/s12598-014-0423-z

RARE METALS
www.editorialmanager.com/rmet

Anode material NbO for Li-ion battery and its electrochemical properties

Jian Li, Wen-Wen Liu, Hong-Ming Zhou*, Zhong-Zhong Liu, Bao-Rong Chen, Wen-Jiao Sun

Received: 11 December 2013 / Revised: 5 January 2014 / Accepted: 27 November 2014 / Published online: 9 January 2015
© The Author(s) 2015. This article is published with open access at Springerlink.com

Abstract The NbO electrode materials were successfully synthesized by high-temperature solid-phase method using Nb powders and Nb_2O_5 powders as raw materials. The crystalline structure, morphology, and electrochemical properties of the obtained materials were characterized by X-ray diffraction (XRD), scanning electron microscopy (SEM), dynamic light scattering instrument (DLSA), half-cell charge–discharge tests, and cyclic voltammetry (CV). The reaction mechanism of lithium with NbO was investigated by ex-situ XRD studies. The results show that material average Li storage voltage is nearly located at 1.6 V, and the lithium intercalation into NbO remains a single-phase process. For the first discharge, a capacity of 355 $mAh{\cdot}g^{-1}$ is obtained at a current rate of 0.1C, and 293 $mAh{\cdot}g^{-1}$ is maintained after 50 cycles, whereas a capacity of 416 $mAh{\cdot}g^{-1}$ is obtained at a current rate of 0.1C after ball milling. And 380 $mAh{\cdot}g^{-1}$ reversible capacity remains for the ball milling sample.

Keywords Niobium oxide; Anode; Electrochemical properties; Lithium-ion batteries

1 Introduction

In recent years, great interest is centered on the development of electronic products such as laptop computers, cellular cameras, and mobile phones. As a result, lithium-ion batteries are widely used in electronic devices and also considered as power sources for large-scale energy storage equipment [1, 2]. In general, graphite is used as the anode material, but its capacity is limited to 372 $mAh{\cdot}g^{-1}$, and the formation of a solid electrolyte interphase (SEI) on the surface of graphite electrodes corresponds to low cycle performance [3–5]. Therefore, attention is directed at the use of binary lithium alloys as an alternative to graphite for anode electrode. Researches on Li–Si [6], Li–Sn [7], Li–Sb [8] were reported. However, the drawback of the lithium alloys is their poor capacity retention during cycling, which limits them for commercial application. Recently, $Li_4Ti_5O_{12}$ becomes a promising candidate for anode electrodes due to its excellent ability that insert/extract Li nearly has no volume change [9]. Nevertheless, the theoretical capacity of $Li_4Ti_5O_{12}$ is only 175 $mAh{\cdot}g^{-1}$, which is inadequate for the large-scale consumption of most devices.

In order to find more competitive anode materials for Li-ion batteries, scholars did a lot of researches. Recently, niobium oxides attract great attention because of niobium alloy's changeable valence state. Niobium oxide was first examined for use as primary lithium cells by Ohzuku et al. [10]. Subsequently, Naoaki et al. [11] reported that Nb_2O_5 was one of the few possible cathode candidates for 2 V rechargeable lithium batteries. Chen et al. discovered that $LiNb_3O_8$ was a novel anode material for lithium batteries [12]. As niobium oxides have low potential to lithium, which is no more than 1.2 V [13], Nb-based compounds can be used as negative electrodes with redox reactions located between 1.0 and 3.0 V [14–19]. As NbO intrinsically has excellent electrical conduction properties, it is widely used as electrode materials for super capacitors. And there are few reports on the use of NbO as an electrode

J. Li, W.-W. Liu, H.-M. Zhou*, Z.-Z. Liu, B.-R. Chen, W.-J. Sun
School of Materials Science and Engineering, Central South University, Changsha 410083, China
e-mail: ipezhm@163.com

J. Li, H.-M. Zhou
Hunan Zhengyuan Institute for Energy Storage Materials and Devices, Changsha 410083, China

for lithium batteries. In this paper, it was reported a novel anode material of NbO as an electrode for lithium batteries by its electrochemical properties.

2 Experimental

2.1 Synthesis and characterization of NbO

The NbO was prepared by a high-temperature solid-phase reduction method. Stoichiometric amounts of high purity (Alfa, 99.9 %) niobium metal powder and Nb_2O_5 (Alfa, 99.9 %) powder were mixed, stirred well, and placed in a tube furnace. The tube was then evacuated and closed. Next, the mixture was heated slowly at a rate of 5 °C·min^{-1} to 1,000 °C and kept under argon atmosphere for 3 h. The NbO powder was obtained after allowing the furnace to cool. The NbO powder was ball-milled in a planetary ball mill with acetylene black in a ratio of 80:10 at 300 r·min^{-1} for 16 h, and the obtained sample was called NbO-BM.

Structural characterization of the sample was done by powder X-ray diffraction (XRD) (D/max 2500 VB, Japan, Cu Kα1 radiation) and scanning electron microscope (SEM, FEI Sirion 200). The distribution of solid particles was determined using a ZetaSizer 3000 dynamic light scattering instrument (DLSA, Malvern Inc.)

2.2 Electrochemical characterization

For electrochemical studies, the NbO electrodes were fabricated using NbO as the active material, acetylene black, and polyvinylidene fluoride (PVDF) as the binder in a weight ratio of 80:10:10. In contrast, an electrode was fabricated without acetylene black by keeping PVDF in the same weight ratio. The weight ratio between NbO-BM and binder was 90:10 for the NbO-BM electrode. The mixture was dissolved in N-methyl pyrrolidone (NMP) solvent to form uniform viscous slurry after stirring. The slurry was coated onto Al foil and dried at 100 °C in vacuum for 12 h. Coin-type test cells (CR 2032) were assembled using the active material as the electrode, Li metal foil as the anode electrode, 1 mol·L^{-1} $LiPF_6$ in 1:1 EC + DMC as the electrolyte, and polypropylene separator in an argon-filled glove box (Siemens, Germany). Charge–discharge cycling and cyclic voltammetry (CV) of cells were carried out in galvanostatic mode at current rates of 0.1C and 0.5C by Neware battery cycling unit (BTS-MPTS, China) and electrochemical workstation (CHENHUA, China) at room temperature, respectively. The test voltage range of the cells is from 1.0 to 3.0 V at scan rates of 0.1 mV·s^{-1}. At various lithiated and delithiated states, the cells were disassembled inside the glove box. The electrodes were covered with a mylar film, and ex-situ XRD patterns were obtained.

3 Results and discussion

3.1 Characterization of materials

Figure 1a shows the XRD patterns of the NbO and NbO-BM samples. All diffraction peaks in both samples can be indexed to the cubic phase (PDF card no. 71-2146). Both the samples belong to the cubic *Pm*3*m* [221] space group with lattice parameters calculated as $a = 0.4210$ nm, $b = 0.4210$ nm, and $c = 0.4210$ nm, which were in agreement with the standard report, indicating that a pure and homogeneous phase NbO is achieved. It can be seen from the (111) crystal plane (Fig 1b) that, the characteristic peak intensity of the NbO-BM sample is slightly lower than that of the NbO, and the peaks of the NbO-BM sample are slightly broader than those of NbO. Compared with the NbO sample, the peak position of the NbO-BM sample

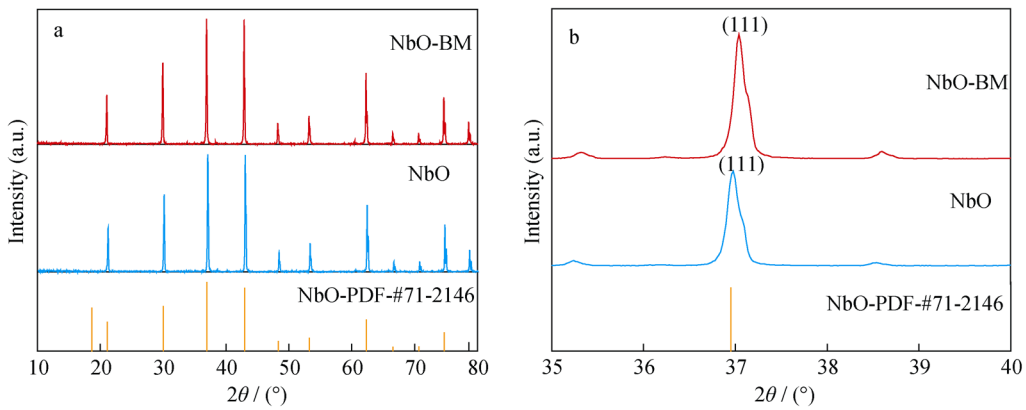

Fig. 1 XRD patterns of **a** NbO, NbO-BM samples and **b** (111) crystal plane of NbO and NbO-BM samples

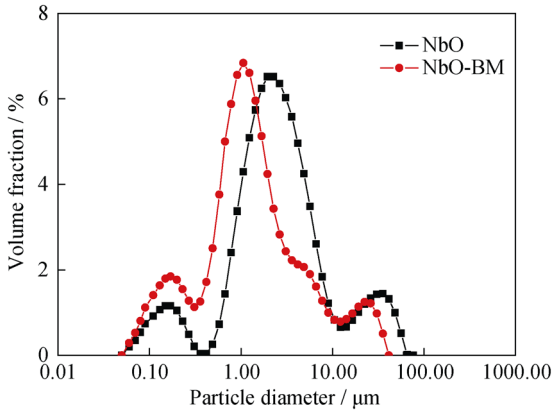

Fig. 2 DLSA patterns of NbO and NbO-BM samples

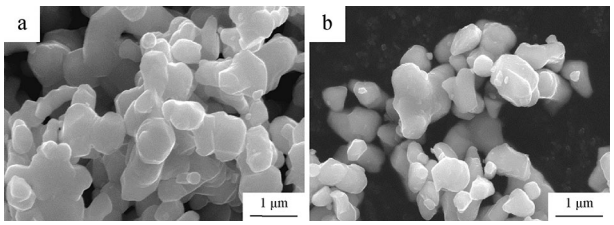

Fig. 3 SEM images of samples: **a** NbO and **b** NbO-BM

shifts markedly. This means that the NbO-BM sample has a smaller particle size, and the lattice structure of the sample has no obvious changes after ball milling.

The particle diameter distributions of NbO and NbO-BM samples are presented in Fig. 2. It can be seen from Fig. 2 that the average particle sizes of NbO and NbO-BM are about 2.57 and 1.28 μm, respectively. And the grain size distribution of NbO-BM is more concentrated, which is attributed to the fact that ball milling could reduce the particle size and also narrow the distribution range of particle size.

The SEM images of the samples are presented in Fig. 3a and b. The SEM investigation reveals that the NbO samples have an average particle diameter of 200–300 nm, and the particles aggregate together to form a larger particle, while the particle size of the NbO-BM sample is smaller and the particles spread more evenly after ball milling, which is consistent with the widening of the XRD patterns.

3.2 Electrochemical property of NbO

The first three CV curves for the NbO electrode are shown in Fig. 4. In the first cycle, the pronounced reduction (Li insertion) peaks could be observed at 1.5 V, while the oxidation (Li extraction) peaks are observed at 1.9 V, which could be related to the reaction transfer of NbO and Li (as discussed below by ex-situ XRD). The large hump reduction and oxidation peaks at 1.5 and 1.9 V do not

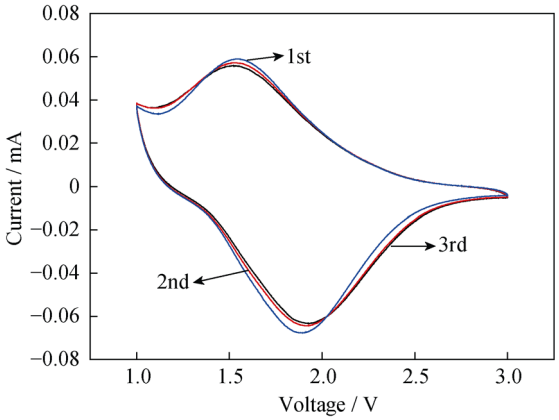

Fig. 4 CV curves of NbO electrode between 1.0 and 3.0 V at a scan rate of 0.1 $mV \cdot s^{-1}$

disappear in the subsequent cycles. This indicates that the structure of NbO can be significantly reversibly changed upon Li insertion. The average lithium storage voltage is approximately 1.6 V by taking the mid-point between the oxidation peak and reduction peak.

Figure 5a, b shows the discharge/charge curves of the NbO and NbO-BM electrode samples. It can be observed that no significant plateaus of initial discharge curves are presented in both samples. The typical sloped feature from 2.0 to 1.2 V is in agreement with CV results. The NbO initial discharge capacity is 355 $mAh \cdot g^{-1}$, and it remains relatively stable with discharge capacity reaching as high as 293 $mAh \cdot g^{-1}$ after 50 cycles. As a reference, the NbO-BM samples demonstrate a higher initial discharge capacity, reaching 416 $mAh \cdot g^{-1}$, and after 50 cycles, it still remains at 380 $mAh \cdot g^{-1}$.

In order to clarify the reaction mechanism of Li with NbO during the first cycle, ex-situ XRD experiments were performed. The XRD patterns shown in Fig. 6 are taken at the steps indicated in Fig. 5. There is no significant change in the XRD patterns from the open-circuit voltage of 2.8 to 1.0 V (Points A–I in Fig. 5). By charging from 1.25 to 3.00 V (Points J–Q in Fig. 5), the XRD patterns still have no obvious changes, which indicates that the lithium intercalation into NbO remains in a single phase, and a biphasic interface does not form in the lithium intercalation/deintercalation process. Upon the first discharging, a large expansion of the lattice parameters changes from $a = b = c = 0.42083$ nm (Point A in Fig. 5) to $a = b = c = 0.42122$ nm (Point I in Fig. 5), which corresponds to lithium ion's intercalation. Upon the first charge, the lattice parameters return to contraction with $a = b = c = 0.4.2117$ nm (Point Q in Fig. 5), corresponding to delithiation process. Based on the discharge/charge, ex-situ XRD and CV results were studied. The lithium ion's intercalation/deintercalation process can be described by the following equation:

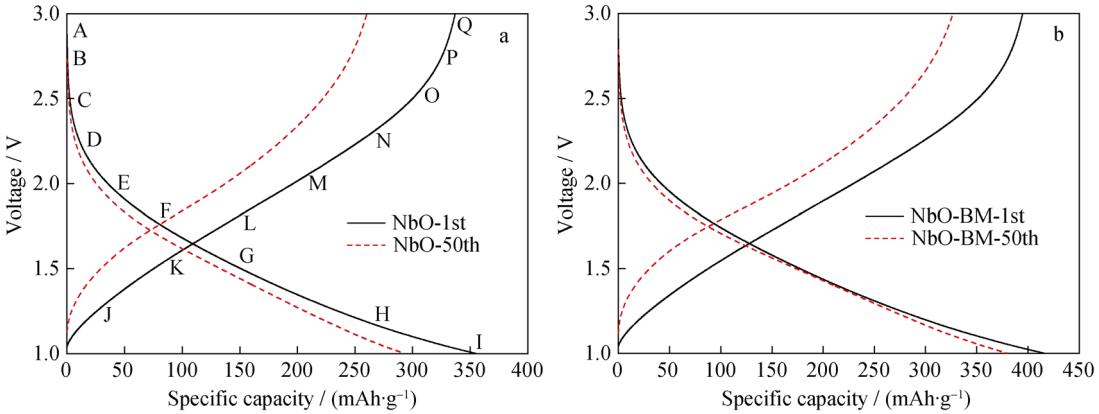

Fig. 5 Capacity–voltage-composition profiles of NbO and NbO-BM electrodes at a current rate of 0.1C: **a** NbO and **b** NbO-BM

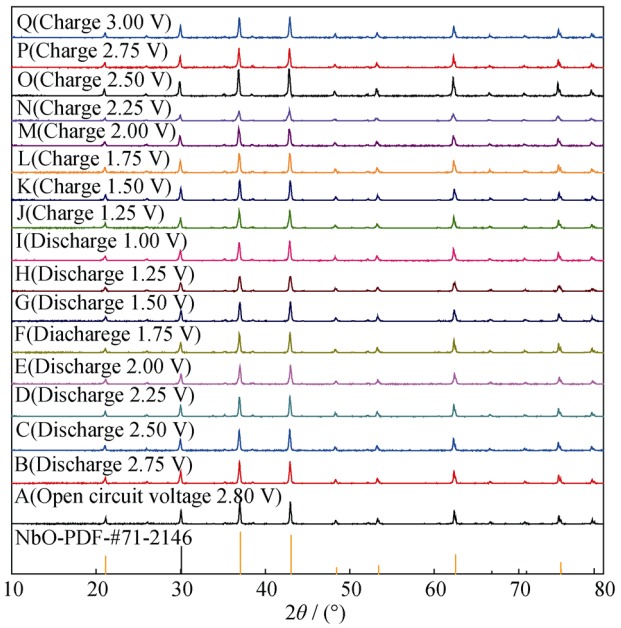

Fig. 6 Ex-situ XRD patterns of Li/NbO cell at various lithiated and delithiated states

$$x\mathrm{Li}^{+} + x\mathrm{e}^{-} + \mathrm{NbO} \leftrightarrow \mathrm{Li}_x\mathrm{NbO} \quad (1)$$

Figure 7 displays the cycling performance of the NbO and NbO-BM electrodes at current rates of 0.1C and 0.5C, respectively. At a current rate of 0.1C, the reversible capacity of the NbO-BM sample is still intact at 380 mAh·g^{-1} after 50 cycles. In contrast, the capacity of the NbO electrode is only 293 mAh·g^{-1}. After the NbO is ball-milled with acetylene black, its capacity can be enhanced by 87 mAh·g^{-1}. When the current rate increases to 0.5C, the improvement is even more obvious. The capacity reaches 216 mAh·g^{-1} for the NbO-BM sample after 50 cycles, while a capacity of only 162 mAh·g^{-1} can be achieved for the NbO sample. The pronounced improvement in Li storage performance

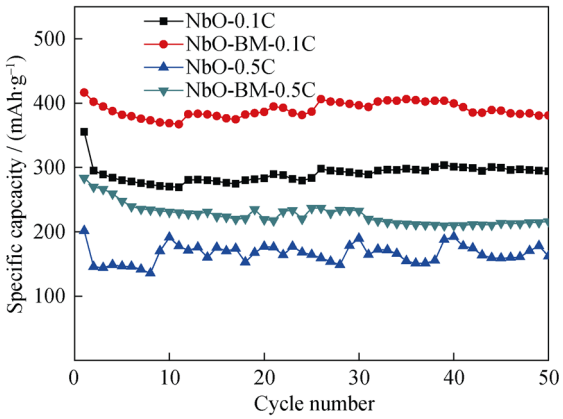

Fig. 7 Cycling performance for both electrodes cycled at current rates of 0.1C and 0.5C

can be attributed to the mixed conducting network and a smaller particle size in the NbO-BM sample.

Figure 8 depicts the curve of charge–discharge capacity variation for the sample without addition of acetylene black and the NbO electrode sample. The initial discharge capacity of the no acetylene black NbO is only 96 mAh·g^{-1}, and decreases to 60 mAh·g^{-1} after 50 cycles. This indicates that the homogeneous distribution of conduct material builds the electronic transport path, and the smaller size of the active material significantly reduces the Li^+ diffusion length. Both samples exhibit good cycling performance after several cycles with high coulombic efficiency, which may be attributed to no SEI formation during the Li insertion/extraction into/from the material in the voltage range of 1.0–3.0 V. In the case of alloy systems, metal oxide decomposes and a thermodynamically stable amorphous Li_2O matrix forms [20, 21]. This causes the problem of irreversible capacity loss. The major origin of irreversible capacity loss at the NbO was not investigated in this article. Further work on the Li storage mechanism in this material is still ongoing.

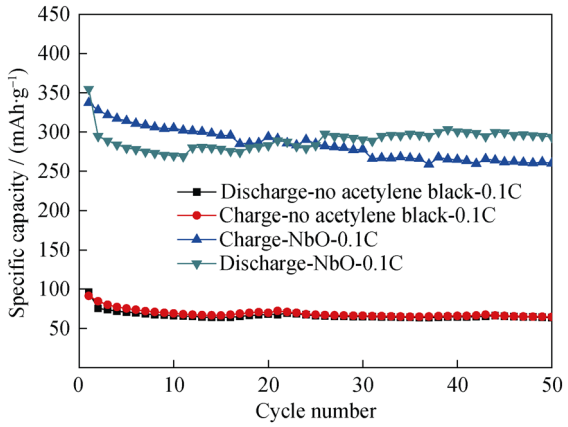

Fig. 8 Charge–discharge capacity variation for 50 cycles

4 Conclusion

Electrochemical studies on NbO as an anode electrode for lithium-ion battery were carried out. The ex-situ XRD patterns taken at the end of each step of discharge and charge indicate that the lithium intercalation into NbO remains a single-phase process. After the NbO is ball-milled with acetylene black, its initial discharge capacity can reach 416 $mAh \cdot g^{-1}$ at a current rate of 0.1C, and the capacity remains 380 $mAh \cdot g^{-1}$ after 50 cycles. The average Li storage voltage is roughly 1.6 V. Results of electrochemical properties show that the NbO electrode has a highly reversible and stable charge/discharge capacity, and may be a good candidate as an anode electrode for lithium-ion battery.

Acknowledgments This work was financially supported by the National Science and Technology Support Project of China (No.2007BAE12B01) and the Science and Technology Project of Changsha (No. k1201039-11).

Open Access This article is distributed under the terms of the Creative Commons Attribution License which permits any use, distribution, and reproduction in any medium, provided the original author(s) and the source are credited.

References

[1] Peter GB. Solid-state chemistry of lithium power sources. Chem Commun. 1997;19:1817.
[2] Armand M, Tarascon JM. Building better batteries. Nature. 2008;451(7179):652.
[3] Wang JQ, Raistrick ID, Huggins RA. Behavior of some binary lithium alloys as negative electrodes in organic solvent-based electrolytes. J Electrochem Soc. 1986;133(3):457.
[4] Ban LQ, Zhuang WD, Lu HQ, Yin YP, Wang Z. Progress in modification of layered cathode material Li–Ni–Co–Mn–O. Chin J Rare Met. 2014;37(5):820.
[5] Smith AJ, Burns JC, Zhao XM. A high precision coulometry study of the SEI growth in Li/graphite cells. J Electrochem Soc. 2011;158(5):A447.
[6] Kim I, Blomgren GE, Kumta PN. Si–SiC nanocomposite anodes synthesized using high-energy mechanical milling. J Power Sour. 2004;130(2):275.
[7] Wen CJ, Huggins RA. Thermodynamic study of the lithium–tin system. J Eletrochem Soc. 1981;128(6):1181.
[8] Li H, Wang Q, Shi LH. Nanosized SnSb alloy pinning on hard non-graphitic carbon spherules as anode materials for a Li ion battery. Chem Mater. 2002;14(1):103.
[9] Nichllas AM, Christopher SG, John VH. Lithium intercalation into the titanosilicate sitinakite. Chem Mater. 2006;18(14):3192.
[10] Ohzuku T, Sawai K, Hirai T. Electrochemistry of L-niobium pentoxide a lithium/non-aqueous cell. J Power Sour. 1987;19(4):287.
[11] Naoaki K, Yoshimasa K, Shinichi K. Thermodynamics and kinetics of lithium intercalation into Nb_2O_5 electrodes for a 2 V rechargeable lithium battery. J Eletrochem Soc. 1999;146(9):3203.
[12] Jian ZL, Xia L, Fang Z, Hu YS, Zhou J, Chen W, Chen LQ. $LiNb_3O_8$ as a novel anode material for lithium-ion batteries. Electrochem Commun. 2011;10(13):1127.
[13] Li H, Palani B, Joachim M. Li-storage via heterogeneous reaction in selected binary metal fluorides and oxides. J Electrochem Soc. 2004;151(11):A1878.
[14] John BG, Youngsik K. Challenges for rechargeable Li batteries. Chem Mater. 2010;22(3):587.
[15] Reddy MA, Varadaraju UV. Facile insertion of lithium into nanocrystalline $AlNbO_4$ at room temperature. Chem Mater. 2008;20(14):4557.
[16] Colin JF, Pralong V, Caignaert V. A novel layered titanoniobate $LiTiNbO_5$: topotactic synthesis and electrochemistry versus lithium. Inorg Chem. 2006;45(18):7217.
[17] Wei MD, Wei KM, Masaki I. Nb_2O_5 nanobelts: a lithium intercalation host with large capacity and high rate capability. Electrochem Commun. 2008;7(10):980.
[18] Pralong V, Reddy MA, Caignaert V. A new form of $LiNbO_3$ with a lamellar structure showing reversible lithium intercalation. Chem Mater. 2011;23(7):1915.
[19] Son JT. Novel electrode material for Li ion battery based on polycrystalline $LiNbO_3$. Electrochem Commun. 2004;10(6):990.
[20] Courtney IA, Dahn JR. Electrochemical and in situ X-ray diffraction studies of the reaction of lithium with tin oxide composites. J Electrochem Soc. 1997;144(6):2045.
[21] Liu W, Huang X, Wang Z, Li H. Studies of stannic oxide as an anode material for lithium-ion batteries. J Electrochem Soc. 1998;145(1):59.